PHYSICAL REVIEW VOLUME 177, NUMBER 5 25 JANUARY 1969

Rescattering Model for $K^- + p \to \Sigma^- + \pi^+$

C. P. SINGH AND B. K. AGARWAL
Physics Department, Allahabad University, Allahabad, India
(Received 16 September 1968)

A rescattering model is proposed which accounts for the experimental angular distributions in the process $K^- + p \to \Sigma^- + \pi^+$.

RECENT experimental study[1] of K^--p reactions, when the incident K^- momentum is in the few-GeV/c region, has revealed anomalous behavior in the angular distributions. It is not possible to understand this behavior within the framework of the single-particle-exchange model. There is a need, therefore, to investigate this phenomenon by going beyond this simple model. The simplest way out would be to consider a rescattering square diagram for such processes.

The anomalous behavior is quite prominent in the reaction [Fig. 1(a)]

$$K^- + p \to \Sigma^- + \pi^+ , \tag{1}$$

for which a backward peak is observed at high energies,[2] but below about 1.5 GeV/c the angular distributions show a forward peaking along with a mild backward peaking.[3,4] The meson exchange being C-forbidden, we must give up the hope of meeting this situation on the basis of one-particle-exchange contributions. In Fig. 2 we show the singularities for reaction (1). If we fix s on the straight line S of Fig. 2, we can determine the singularities. We have, e.g., a cut at $t = (m_\pi + m_K)^2$, a pole at $u = m^2$, i.e., $t = \sum m_i^2 - m^2 - s$, and a cut from $u = (m + m_\pi)^2$, i.e., $t = \sum m_i^2 - (m + m_\pi)^2 - s$. We therefore assume that (1) is dominated by a two-particle-exchange graph [Fig. 1(b)] which contributes the nearest singularity in the t variable. We further assume that at the energy involved, this diagram can be approximated by the rescattering square diagram shown in Fig. 3. We now put the s-channel particles on the mass shell, which implies that the reaction (1) is a two-step process:

$$K^- + p \to \rho^0 + \Lambda \to \Sigma^- + \pi^+ . \tag{2}$$

This will enable us to extract a convergent contribution from Fig. 3 by using Hamilton's coincident-pole method.[5,6] In this method it is possible to write the fourth-order matrix element as a product of two matrix elements corresponding to the two successive second-order processes (2).

Using the masses and the momenta of the particles as labeled in Fig. 3, we can write the invariant ampli-

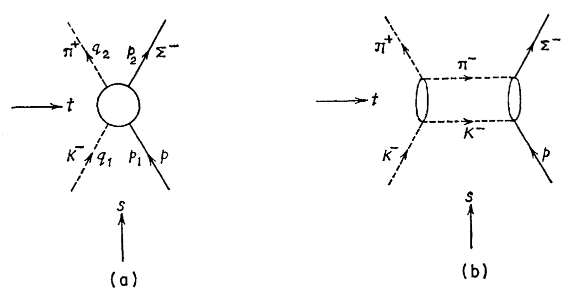

FIG. 1. (a) Labeling of momenta of the particles for the reaction $K^- + p \to \Sigma^- + \pi^+$. (b) Two-meson-exchange diagram for the reaction $K^- + p \to \Sigma^- + \pi^+$.

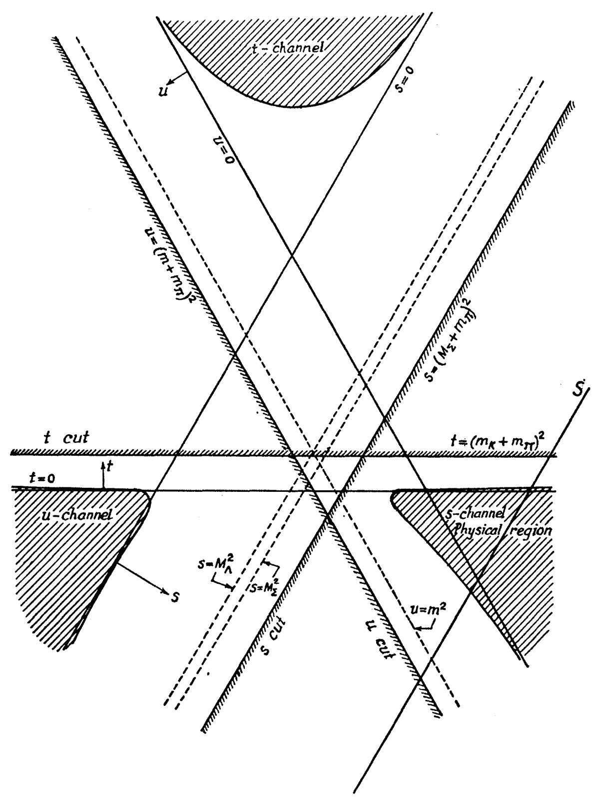

FIG. 2. Locations of the important singularities to the $\Sigma^-\pi^+$ production amplitude with respect to the physical regions are indicated in the Mandelstam diagram, which is drawn approximately to scale.

[1] L. Lyons, Nuovo Cimento **43A**, 888 (1966).
[2] Birmingham-Glasgow-London (I.C.)-Oxford-Rutherford Collaboration, Phys. Rev. **152**, 1148 (1966).
[3] W. A. Cooper *et al.*, in *Proceedings of the International Conference on High-Energy Physics, Geneva, 1962*, edited by J. Prentki (CERN Scientific Information Service, Geneva, 1962), p. 298.
[4] P. M. Dauber, P. E. Schlein, W. A. Slater, D. H. Stork, and H. K. Ticho, Phys. Letters **23**, 154 (1966).
[5] J. Hamilton, Proc. Cambridge Phil. Soc. **48**, 640 (1952).
[6] C. P. Singh and B. K. Agarwal, Phys. Rev. **173**, 1611 (1968); Nuovo Cimento **54A**, 497 (1968).

tude[7] as

$$T_4 = \int \frac{d^4p'}{(2\pi)^4} \bar{u}(p_2) g_{\Lambda\pi\Sigma}\gamma_5 \frac{-i\gamma\cdot p' + M_\Lambda}{p'^2 + M_\Lambda^2} \gamma_5 g_{\bar{K}p\Lambda} \times \frac{1}{Q_1^2 + M_K^2} i g_{\rho K\bar{K}} (q_1 + Q_1)_\mu \frac{\delta_{\mu\nu} + q_\mu' q_\nu'/m_\rho^2}{q'^2 + m_\rho^2} \times i g_{\rho\pi\pi}(q_2 - Q_2)_\nu \frac{1}{Q_2^2 + m_\pi^2} u(p_1). \quad (3)$$

It is possible to find a value of p' for which both the denominators $p'^2 + M_\Lambda^2$ and $q'^2 + m_\rho^2$ vanish. This corresponds to the situation in which ρ^0 and Λ are free particles. The coincident-pole contribution can be extracted by integrating over p_0', which gives a pole (i.e., a δ-function) contribution from the first denominator. Now we substitute the value

$$p_0' = \pm[(\mathbf{p}'^2 + M_\Lambda^2)^{1/2} - i\eta]$$

(where $\eta > 0$) in the second denominator and take the pole (or δ-function) contribution over the remaining integration. The process (1) is now a two-step process (2) for which we can write

$$\langle p_2, q_2 | T_4 | p_1, q_1 \rangle = \frac{1}{2}\int \frac{d^3p'}{(2\pi)^3} \frac{d^3q'}{(2\pi)^3} \frac{M_\Lambda}{p_0'} \frac{1}{2q_0'} \langle p_2, q_2 | T_2 | p', q' \rangle \times \langle p', q' | T_2 | p_1, q_1 \rangle$$

$$= \frac{1}{4}\int d\cos\theta' \frac{|\mathbf{q}'| M_\Lambda}{2\pi W} \bar{u}(p_2) g_{\Lambda\pi\Sigma}\gamma_5 \frac{1}{Q_2^2 + m_\pi^2} \times \frac{-i\gamma\cdot p' + M_\Lambda}{2M_\Lambda} \gamma_5 g_{\bar{K}p\Lambda} i g_{\rho\pi\pi}(q_2 - Q_2)_\nu \times \left(\delta_{\mu\nu} + \frac{q_\mu' q_\nu'}{m_\rho^2}\right) i g_{\rho K\bar{K}} (q_1 + Q_1)_\mu \frac{1}{Q_1^2 + m_K^2} \times u(p_1), \quad (4)$$

where W is the c.m. total energy and $\cos\theta' = \hat{q}_1 \cdot \hat{q}'$. To evaluate the integral in (4) we use the fact[8] that the function $F = 1/(Q_1^2 + m_K^2)(Q_2^2 + m_\pi^2)$ is a rapidly varying function of $\cos\theta'$, and therefore essentially determines the angular distribution. Hence, we substitute in the rest of the integrand that value of $\cos\theta'$ for which the function F is maximum (i.e., $\cos\theta' \rightarrow 1$).

[7] We have adopted the notations of J. D. Jackson and H. Pilkuhn, Nuovo Cimento **33**, 906 (1964).

[8] L. Bertocchi and A. Capella, Nuovo Cimento **51A**, 369 (1967).

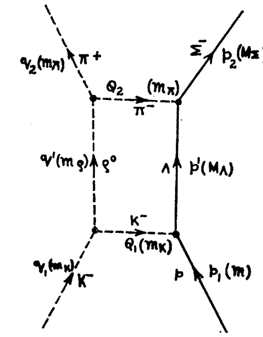

FIG. 3. Rescattering diagram for $K^- + p \rightarrow \Sigma^- + \pi^+$.

This allows us to write[9]

$$T_4 = \frac{Y|\mathbf{q}'|}{8\pi W} \bar{u}(p_2) g_{\Lambda\pi\Sigma}\gamma_5(-i\gamma\cdot p' + M_\Lambda)\gamma_5 g_{\bar{K}p\Lambda} \times i g_{\rho\pi\pi}(q_2 - Q_2)_\nu \left(\delta_{\nu\mu} + \frac{q_\nu' q_\mu'}{m_\rho^2}\right) i g_{\rho K\bar{K}}(q_1 + Q_1)_\mu \times u(p_1), \quad (5)$$

where

$$Y = \frac{1}{8|\mathbf{q}_1||\mathbf{q}'^2||\mathbf{q}_2|} \frac{1}{\sqrt{(-\beta)}} \ln \frac{\alpha_1\alpha_2 - \cos\theta_2 + \sqrt{(-\beta)}}{\alpha_1\alpha_2 - \cos\theta_2 - \sqrt{(-\beta)}},$$

$$\beta = 1 - \cos^2\theta_2 - \alpha_1^2 - \alpha_2^2 + 2\alpha_1\alpha_2\cos\theta_2,$$

$$\alpha_1 = \frac{2q_{10}q_0' - m_\rho^2}{2|\mathbf{q}_1||\mathbf{q}'|},$$

$$\alpha_2 = \frac{2q_{20}q_0' - m_\rho^2}{2|\mathbf{q}_2||\mathbf{q}'|},$$

and

$$\cos\theta_2 = \hat{q}_2 \cdot \hat{q}_1.$$

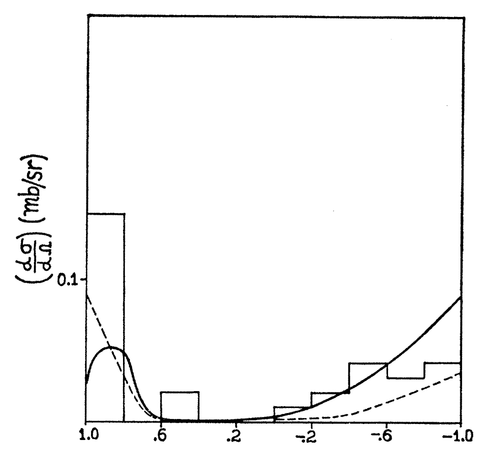

FIG. 4. Production angular distribution in the reaction (1) at a K^- momentum of 1.46 GeV/c. The solid curve is the theoretical prediction yielded by Eq. (6). The dashed curve is the outcome when we assume forward production of ρ^0. The histogram represents the experimental data of Cooper *et al.* (Ref. 3).

[9] A. O. Barut, *The Theory of the Scattering Matrix* (The Macmillan Company, New York, 1967), p. 119.

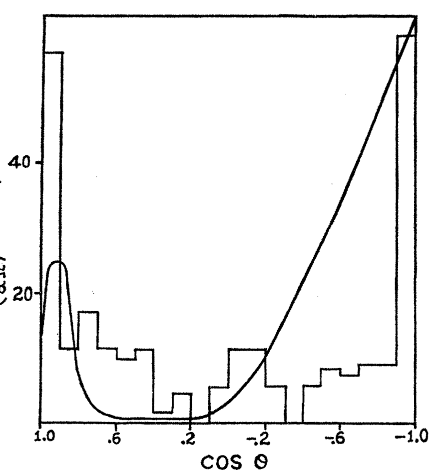

FIG. 5. Production angular distribution at an incident K^- momentum of 1.95 GeV/c. The curve represents the theoretical prediction from Eq. (6). The histogram represents the experimental data of Dauber *et al.* (Ref. 4).

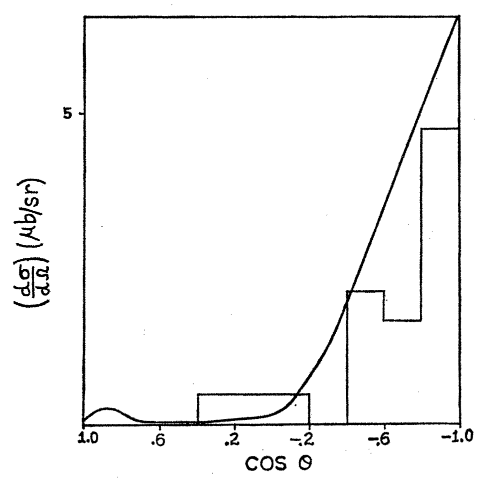

FIG. 6. Production angular distribution at a K^- momentum of 3.5 GeV/c. The curve represents the theoretical prediction from Eq. (6). The histogram represents the experimental data of Ref. 2.

After taking the usual sum over polarization and spin states, we find the differential cross section to be

$$\frac{d\sigma}{d\Omega}=0.38935\frac{mM_\Sigma}{128(2\pi W)^4}|\mathbf{q}'|^2\frac{|\mathbf{q}_2|}{|\mathbf{q}_1|}Y^2g_{\Lambda\pi\Sigma}{}^2g_{\bar{K}p\Lambda}{}^2 \times g_{\rho\pi\pi}{}^2g_{\rho K\bar{K}}{}^2F_1F_2 \text{ mb/sr}, \quad (6)$$

where

$$F_1=16[q_2\cdot q_1+(q_2\cdot q')(q_1\cdot q')/m_\rho{}^2]^2,$$
$$F_2=(2/mM_\Sigma)(mM_\Lambda+p_1\cdot p')(M_\Lambda M_\Sigma+p_2\cdot p').$$

To evaluate the differential cross section from Eq. (6), we take the values of the coupling constants as follows[10,11]: $g_{\Lambda\pi\Sigma}{}^2/4\pi=3.8$, $g_{\bar{K}p\Lambda}{}^2/4\pi=7.4$, and $g_{\rho\pi\pi}{}^2/4\pi=2g_{\rho K\bar{K}}{}^2/4\pi=2.4$. Thus, we have no free parameters in our calculation.

Results of our calculations are shown in Figs. 4–6 along with the experimental histograms. We find that the present calculation is able to account for the forward and backward peaking observed[3] at an incident K^- momentum of 1.46 GeV/c. We are also able to get the correct high-energy behavior[2] (increase in backward peaking) as shown in Figs. 3 and 4.

If we assume[6] forward production of ρ^0 in the intermediate states, that is, if we put $\cos\theta'=1$ in the function F as well, we get the dashed curve shown in Fig. 4. Slight improvement in the agreement with the experimental data shows that this approximation is reasonable.

Thus, we find that the situation created (i) by the presence of both forward and backward peaking and (ii) by the change in the production angular distributions with the change in the incident momenta can be understood in terms of the rescattering diagram.

ACKNOWLEDGMENTS

We are deeply grateful to Professor J. Hamilton for his valuable comments regarding Eqs. (2) and (4), without which we could not have arrived at the present form of the paper. One of us (C.P.S.) is grateful to the Council of Scientific and Industrial Research, New Delhi, and the University Grant Commission for financial assistance.

[10] R. H. Graham, S. Pakvasa, and K. Raman, Phys. Rev. **163**, 1774 (1967).

[11] A. W. Martin and K. C. Wali, Phys. Rev. **130**, 2455 (1963).